# CEBAF PROPOSAL COVER SHEET

This Proposal must be mailed to:

CEBAF
Scientific Director's Office
12000 Jefferson Avenue
Newport News, VA 23606

and received on or before OCTOBER 30, 1989

A. TITLE: STUDY OF THE QUASIELASTIC (e,ép) REACTION IN $^{16}$O AT HIGH RECOIL MOMENTUM

B. CONTACT PERSON: ROBERT LOURIE

ADDRESS, PHONE AND BITNET:

Department of Physics
University of Virginia
Charlottesville, VA 22901

(804)924-6809
LOURIE@VIRGINIA

C. THIS PROPOSAL IS BASED ON A PREVIOUSLY SUBMITTED LETTER OF INTENT

[X] YES
[ ] NO

IF YES, TITLE OF PREVIOUSLY SUBMITTED LETTER OF INTENT

same as above
LOI 88-59

D. ATTACH A SEPARATE PAGE LISTING ALL COLLABORATION MEMBERS AND THEIR INSTITUTIONS

==========

(CEBAF USE ONLY)

Letter Received 10-30-89

Log Number Assigned PR-89-003

By KES

contact: Lourie

# Study of the Quasielastic (e,e′p) Reaction in $^{16}$O at High Recoil Momenta


THE HALL A COLLABORATION

*American University, Cal. State University LA, Case Western Reserve and LANL*
*Continuous Electron Beam Accelerator Facility*
*George Washington University, University of Georgia, Indiana University Cyclotron Facility*
*Kent State University, University of Maryland, Massachusetts Institute of Technology*
*University of New Hampshire, National Institute of Science and Technology*
*Norfolk State University, University of Regina, University of Rochester*
*University of Saskatchewan, Rutgers University, Stanford University*
*University of Virginia, University of Washington, College of William and Mary*
*NIKHEF-K, CEN Saclay, University of Clermont-Ferrand*
*INFN Sezione Sanita, University of Lund*

Spokespersons: R.W. Lourie (UVa), W. Bertozzi (MIT)
L. Weinstein (MIT), A. Saha (CEBAF)



We propose to make a detailed study of the $^{16}$O(e,e′p) reaction to determine the high-momentum content of the nuclear wavefunction and to test several ideas that form our basic phenomenology of (e,e′p). Structure function separations will be made at high recoil momenta in non-parallel kinematics for a broad range of momentum transfer and outgoing proton energies. The high-momentum structure of $^{16}$O would be determined both for the $1p_{3/2}$ and $1p_{1/2}$ spin-orbit partners and in the missing energy continuum.

## Introduction

A topic of particular interest in nuclear physics is the high momentum structure of nuclei. We know that whatever high momentum components exist arise from short-range aspects of the nucleon-nucleon interaction. These components are conspicuously absent in mean field wavefunctions based on potential models. Indeed, in one of the few cases where high recoil momenta have been probed, deuteron (e,e'p)[1] at 500 MeV/c, significant contributions from non-nucleonic degrees of freedom (meson exchange currents and isobar configurations) are required to adequately describe the data. However, proton momentum distributions for single-particle and continuum states in light nuclei are only known for initial momenta $\vec{k}$ <300 MeV/c. Knowledge of the distributions out to much higher initial momenta will provide stringent constraints on nuclear structure models and yield quantitative information on the part of the wavefunction not described by the mean field. Furthermore, one hopes to test whether our conventional nucleon-meson framework continues to provide an adequate description when the relevant distance scale becomes considerably less than the nucleon radius.

A first goal of our program is therefore to establish the high-momentum content of $^{16}$O, both in the single-particle states and in the continuum. The initial measurements will be done at a four-momentum transfer of 0.58 (GeV/c)$^2$ which, while fairly modest, is still significantly larger than can be achieved at present-day facilities. We note that conventional single-particle wavefunctions have little strength for $|\vec{k}| > 500$ MeV/c so a first measurement needs to be made simply to characterize the single-particle strength at these high momenta. It would be surprising indeed if the simple Woods-Saxon potential produced a correct description of the short-range structure of these wavefunctions. Our initial studies will determine the feasibility of more extensive investigations.

The single-particle states, the $1p_{3/2}$ and $1p_{1/2}$, are of particular interest as they are spin-orbit partners and the nuclear spin-orbit force remains to be fully understood on a microscopic basis. This force certainly has its origins in the $\vec{L} \cdot \vec{S}$ part of the NN interaction. This in turn results, in boson exchange models, from $\rho$ and $\sigma$ exchange. We intend to make large variations in $Q^2$ and this variation, along with separation of individual structure functions, should shed light on the contributions to the spin-orbit force. More generally, the structure of these single-particle states, probed at high $Q^2$ and initial momenta, will provide an exceptionally stringent test of any nuclear mean-field theory.

Previous measurements of the single-particle states, including the spin-orbit partners, have been performed at Saclay[2] and NIKHEF.[3] The missing energy spectra obtained in these experiments are shown in figure 1. The greater resolution of the NIKHEF data, and the consequent observation of other, weak states is immediately obvious. These weaker states are thought to arise from multiparticle-multihole configurations in the ground state, giving rise to a non-zero population of the 2s-1d shell. They will be resolved in our proposed CEBAF experiment as well. In both the previous measurements, the initial momentum sampled was limited to being $\leq 300$ MeV/c while only a rather modest maximum $Q^2$ of was obtained.

The short-distance (high-momentum) structure of the nuclear many-body wavefunction

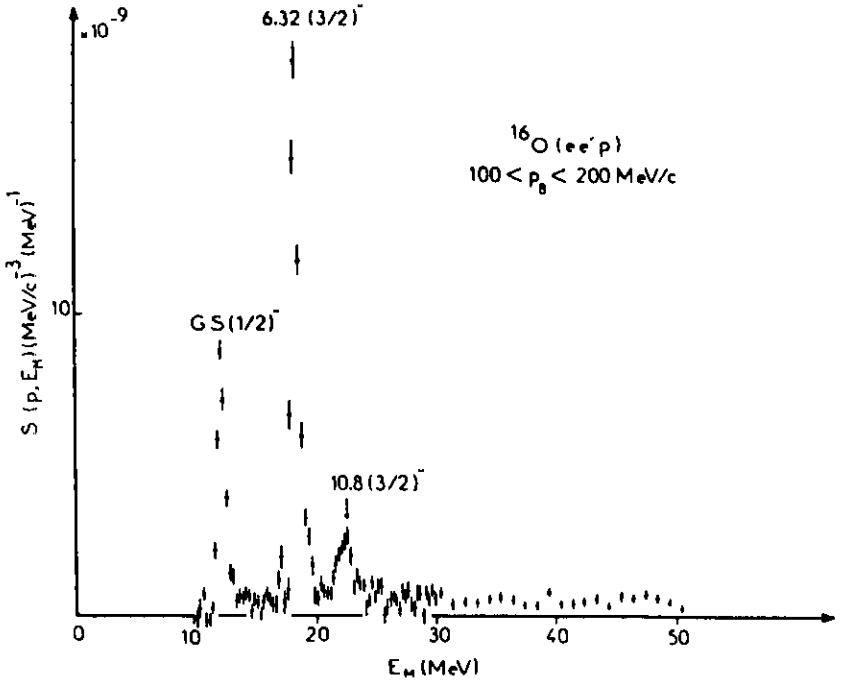


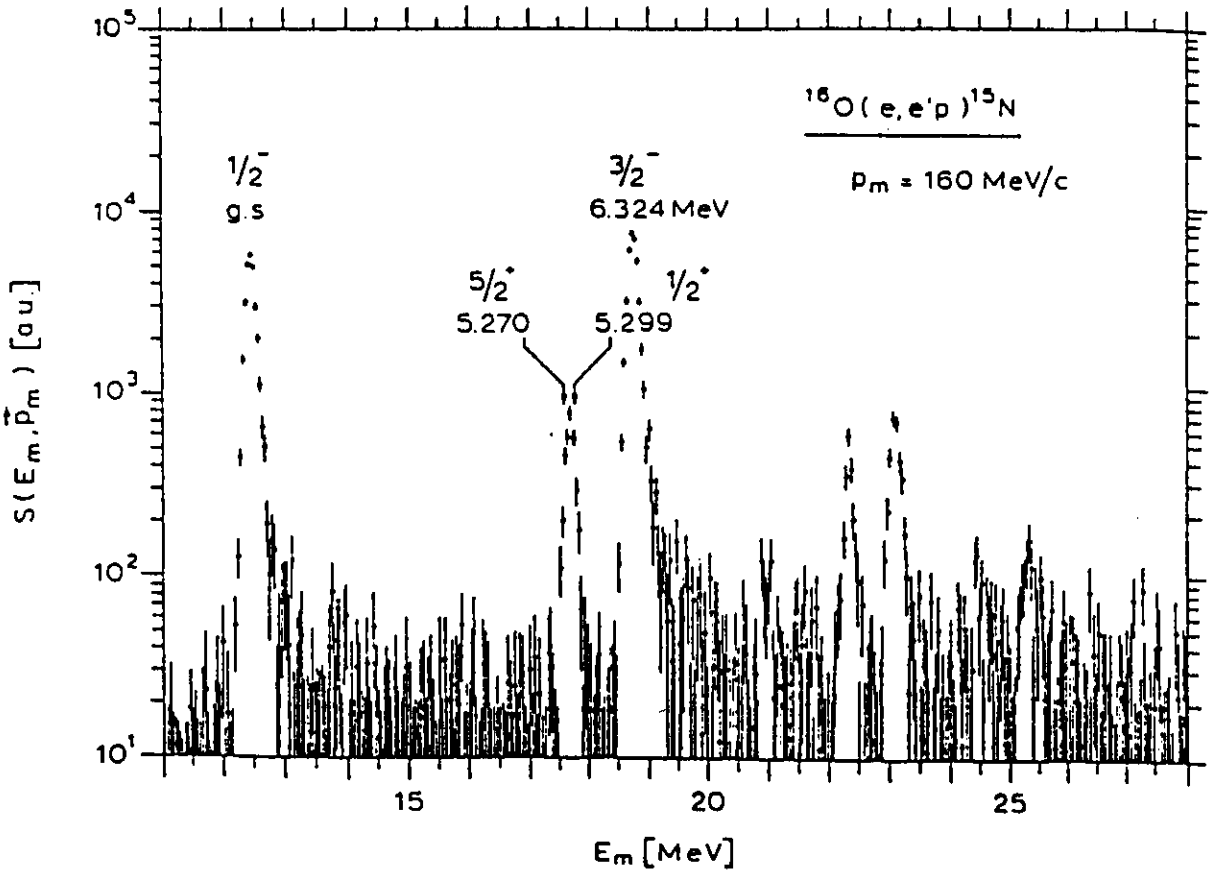


**Figure 1.** *Missing energy spectra for $^{16}O(e,e'p)$ obtained at Saclay (top) and NIKHEF (bottom).*

is, as mentioned above, expected to be significantly affected by the short-range nucleon-nucleon dynamics. In particular, one expects dynamical short-range correlations between nucleons which would be absent in an independent particle model of the nucleus. The search for experimental evidence for these short-range correlations has, until recently, been somewhat frustrating. Calculations of two-body correlations [4] show that they have a dramatic effect on the nucleon momentum distribution $n(\vec{k})$, producing strength at high (>500 MeV/c) momenta which is orders of magnitude greater than in independent particle models (IPMs). This results from the fact that the momentum distribution is directly related to the density correlation function:

$$n(\vec{k}) = \frac{1}{A(2\pi)^3} \int d\vec{r}\, d\vec{r}\,' \, e^{i\vec{k}\cdot(\vec{r}-\vec{r}\,')} \rho_1(\vec{r},\vec{r}\,') \quad , \tag{1}$$

where $\rho_1(\vec{r},\vec{r}\,')$ is the one-body density:

$$\rho_1(\vec{r},\vec{r}\,') = \int d\vec{r}_2 \ldots d\vec{r}_A \, \Psi_A^*(\vec{r},\ldots,\vec{r}_A)\, \Psi(\vec{r}\,',\ldots,\vec{r}_A) \quad , \tag{2}$$

and $\Psi_A$ is the A-body nuclear wavefunction.

Several authors, employing a wide variety of many-body calculational techniques, find that the high-momentum content of nuclei is indeed dominated by two-nucleon correlations. These approaches include sophisticated microscopic (Brueckner-Hartree-Fock),[4] the coherent fluctuation model [5] as well as more phenomenological approaches. [6] Figure 2 shows the nucleon momentum distribution for $^{16}$O as calculated by several of the abovementioned authors and indicates the commonality of the obtained results. In figure 3 we display the calculations of Van Orden *et al.*[5b] using both the Reid soft-core and de Tourreil-Sprung potentials along with the results of Traini and Orlandini[5a] using phenomenological short-range (Jastrow) and longer-range tensor correlations. The latter type results in a D-state component in the pair wavefunction. The harmonic oscillator (HO) and Woods-Saxon (WS) IPM predictions are also displayed. One sees that the correlated distributions completely dominate above 500 MeV/c and that the longer range tensor correlations, though sizeable, are less important than the short-range ones. Clearly, experimental determination of the nucleon momentum distribution should provide the long-sought after direct evidence of short-range correlations.

It is important to note that nuclear structure calculations incorporating two-body correlations [7] predict that much of the high-momentum strength resides in the continuum of the A−1 system, with hundreds of times greater strength than in conventionally treated discrete states. This relationship between high-momentum components and continuum strength has been confirmed by recent measurements of $^3$He(e,e′p) and $^4$He(e,e′p) at Saclay. [8] Their results are displayed in figure 4. One sees that the high $|\vec{k}|$ strength is indeed spread over a large continuum in missing energy and resides mostly in the many-body breakup channels. This basic feature, resulting essentially from the interaction with a correlated nucleon pair, is expected to hold in heavier nuclei as well.

## The (e,e′p) Reaction and Nucleon Momentum Distributions

The (e,e′p) reaction is well-suited for the study of the nucleon momentum distribution. Indeed, most of our current knowledge on $n(k)$, from the deuteron to $^{208}$Pb, has been

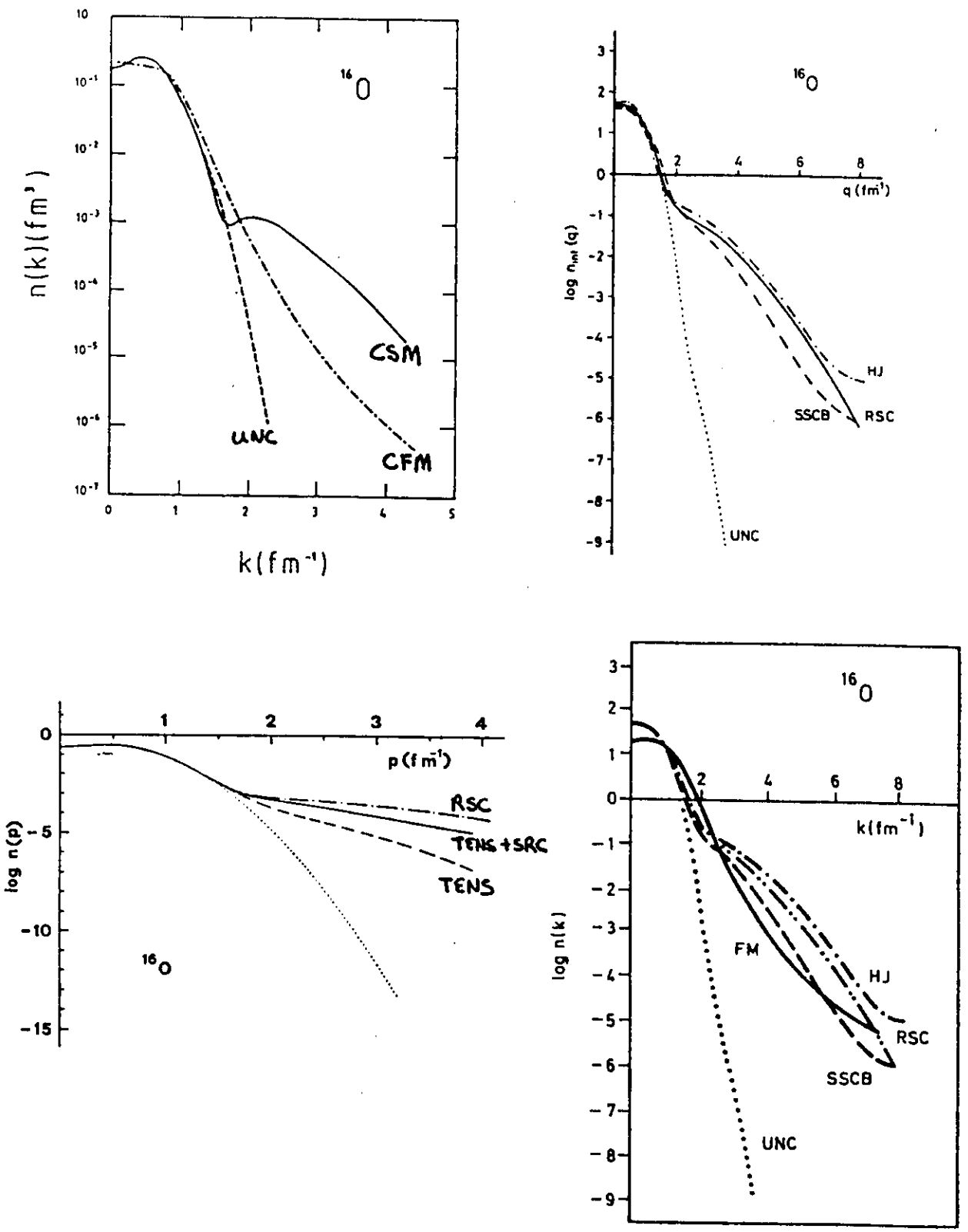


**Figure 2.** *Momentum distributions for $^{16}O$ resulting from several many-body calculations that include short-range correlations. UNC: uncorrelated, CFM: coherent fluctuation model, CSM: correlated shell model. HJ, RSC, SSCB refer to the Hamada-Johnston, Reid soft-core and de Tourreil-Sprung soft core B potentials respectively.*

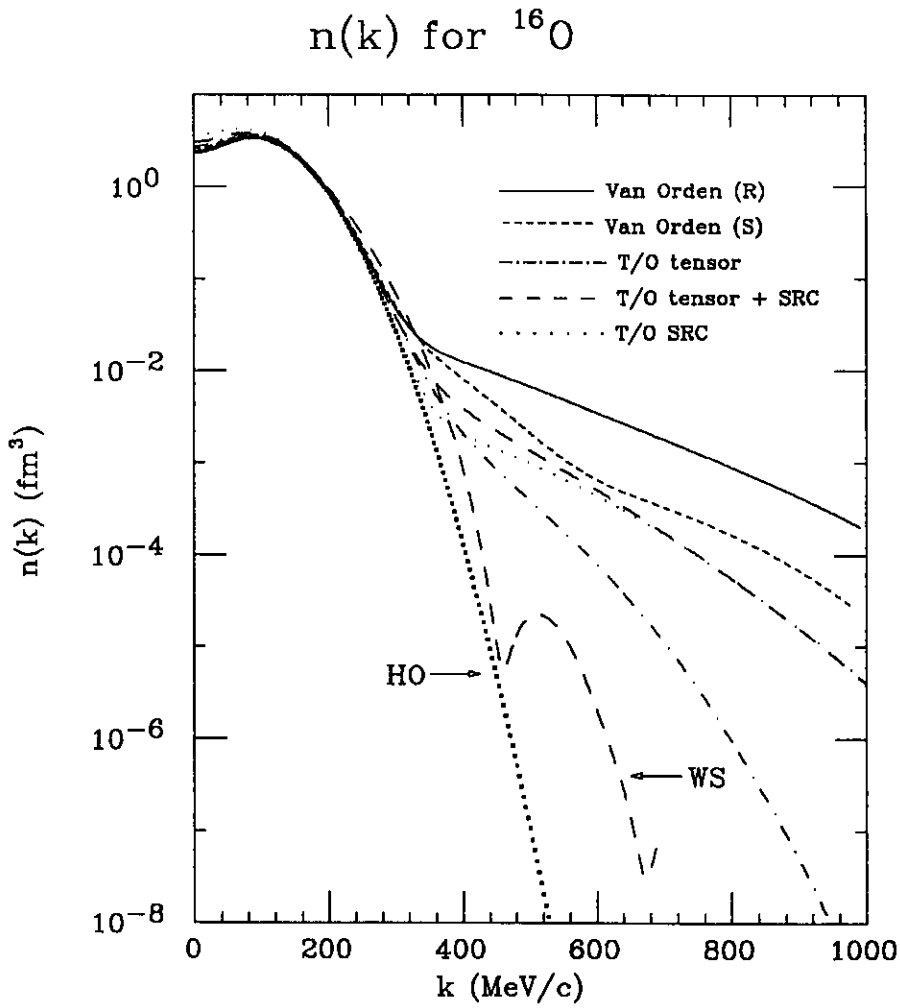


**Figure 3.** *Momentum distributions for $^{16}O$. Various correlated distributions[5] are shown along with single-particle model harmonic oscillator and Woods-Saxon shapes. The influence of short-range and tensor correlations are shown separately.*

obtained via (e,e′p). The (e,e′p) cross section contains four nuclear structure (response) functions when the beam and target are unpolarized and no final state polarizations are observed. These are the longitudinal ($R_L$), the transverse ($R_T$), the longitudinal-transverse interference ($R_{LT}$) and the transverse-transverse interference ($R_{TT}$):

$$\frac{d^4\sigma}{d\Omega_e d\Omega_p d\omega dT_p} = \sigma_M \left(v_L R_L + v_T R_T + v_{LT} R_{LT} \cos\phi_x + v_{TT} R_{TT} \cos 2\phi_x\right) \quad . \tag{3}$$

Three of the response functions can be separated by measurements in the (e,e′) plane where the electron scattering angle $\theta_e$ and the angle $\phi_x$ are varied (to determine $R_{TT}$ requires going out-of-plane). In the plane wave impulse approximation (PWIA), where all of the energy and momentum are assumed to be absorbed on a single quasifree proton, the coincidence (e,e′p) cross section is directly related to $n(\vec{k})$. In this approximation, the (e,e′p) cross section may be written as:

$$\frac{d^4\sigma}{d\Omega_e d\Omega_p d\omega dT_p} = K\sigma_{ep} S(\vec{k},\epsilon) \quad , \tag{4}$$

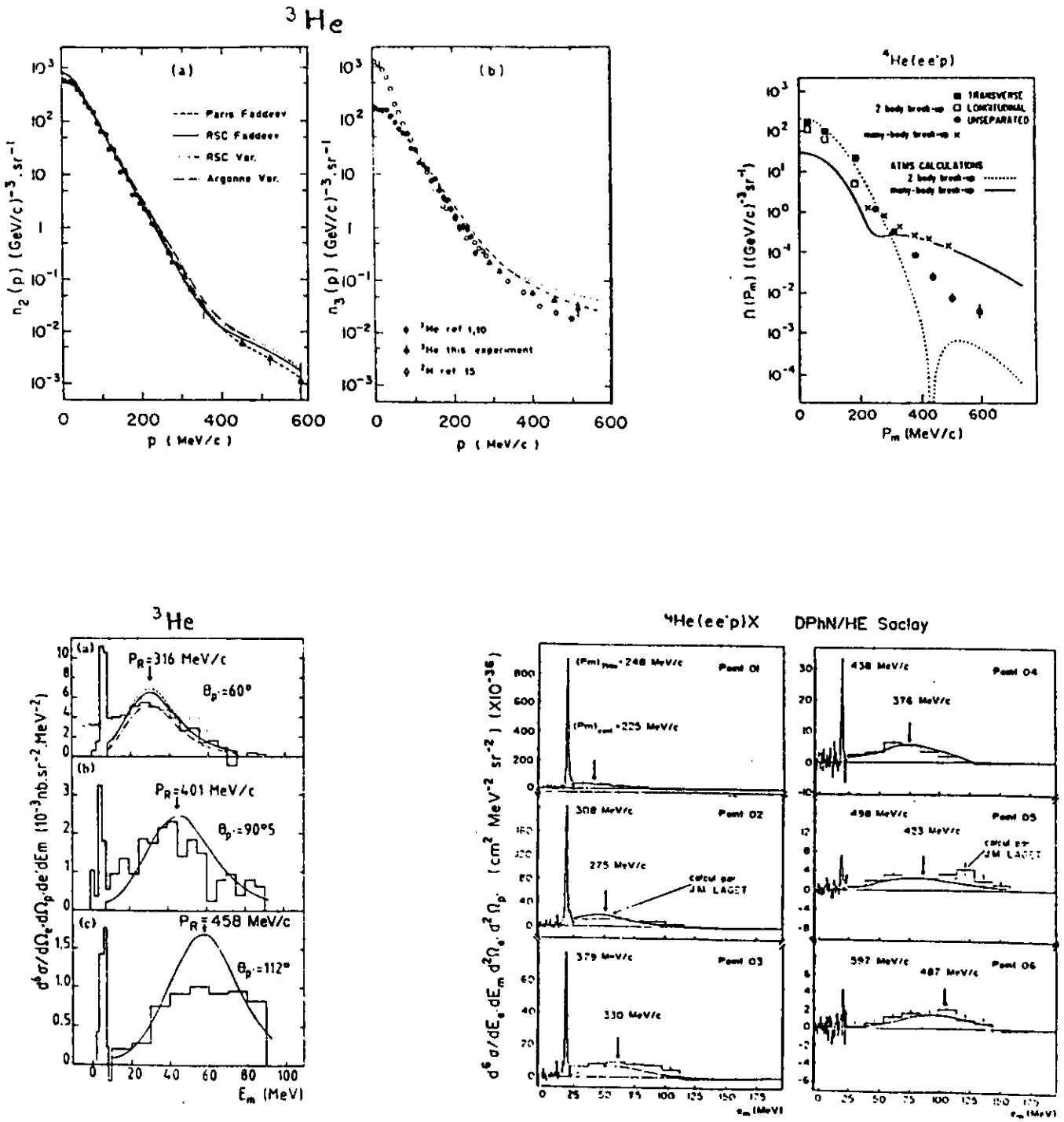


**Figure 4.** *a) The experimental proton momentum distribution in $^3$He and $^4$He from Saclay. Note the dominance of the many-body breakup channels. b) The missing energy spectra obtained in the $^{3,4}$He(e,e'p) reactions. The many-body breakup modes are responsible for the continuum of missing energies.*

where $\sigma_{ep}$ is the cross section for electron scattering from a proton of momentum $\vec{k}$ (which contains the four *nucleon* structure functions) and $S(\vec{k},\epsilon)$, the nuclear spectral function, is the joint probability of finding a proton of momentum $\vec{k}$ within the nucleus and leaving the residual system excited by energy $\epsilon$. The momentum distribution is related to $S(\vec{k},\epsilon)$ by:

$$n(\vec{k}) = \int_0^\infty d\epsilon\, S(\vec{k},\epsilon) \quad . \tag{5}$$

One can partition $S(\vec{k},\epsilon)$ into contributions from bound and continuum states of the residual system:[9]

$$S(\vec{k},\epsilon) = \sum_\alpha |\phi_\alpha(\vec{k})|^2 \delta(\epsilon - \epsilon_\alpha) + n_c(\vec{k}) f(\epsilon) \quad , \tag{6}$$

where, in the IPM, $\phi_\alpha$ is the single-particle wavefunction of the bound state with quantum numbers $\alpha = \{n, \ell, j, \ldots\}$ and $f(\epsilon)$ describes the distribution of the continuum strength over excitation energy. Except in the few-body systems, $f(\epsilon)$ is virtually unknown. One sees that to experimentally determine the high-momentum content of a nucleus involves measuring the (e,e'p) reaction both to discrete and continuum states of the residual system. If the IA were strictly valid, the same momentum distribution appears in each of the four nuclear structure functions. The presence of other reaction components (short-range charged meson exchanges or coupled-channels effects in the reaction process for example) can be detected when the structure functions are separated.

This interesting regime of large nucleon momenta is barely accessible to present electron accelerators. The available incident energy and signal-to-noise problems due to the small cross sections involved and the low ($\sim 1\%$) duty factor of current-day machines pose severe limitations. Except for the few-body systems (the deuteron, Helium-3 and Helium-4) where momenta up to 500 MeV/c have been probed[3,8][10] knowledge of $n(k)$ is restricted to $|\vec{k}|$<300 MeV/c. It is important to realize that these studies were not only been restricted to quite low momentum transfers ($Q^2 \sim 0.05$ (GeV/c)$^2$) but were forced by the limitations of present machines to small values of Bjorken $x$ (0.1–0.2), i.e. to *well beyond the quasielastic peak, into the dip and delta regions.*

CEBAF is uniquely suited for extending these studies on all nuclei to 500 MeV/c and beyond *while maintaining the quasielastic scattering condition* $\omega \approx Q^2/2M$. This lets us select a region where the single-particle physics is suppressed due to the high initial momenta yet the *electron* kinematics still prefer coupling to a single quasifree nucleon. This choice should enhance the importance of competing reaction processes (meson exchanges, isobar currents etc.). Their role, particularly in quasielastic kinematics, is an important open question and one that the measurements proposed here can address. With the greatly extended kinematic range available at CEBAF, we will subject our standard phenomenology of (e,e'p) to much more rigorous tests. This conventional framework for understanding quasielastic (e,e'p) is that:

1) The same momentum distribution appears in all the response functions.

2) The distortion effects can be accounted for simply by a final state optical potential.

3) The one-body interaction is correctly described by an off-shell e-p cross section employing free space form factors.

4) Extranucleonic currents are summarized by meson exchanges and short-range spatial correlations, i.e. that no explicit modification of the nucleon is required.

The relative importance of these different aspects can be varied by making large changes in the momentum transfers and outgoing proton energy and by isolating individual response functions. For example, the elementary e-p cross section depends strongly on momentum transfer while the optical potential is primarily determined by the proton energy. In addition, longitudinal, transverse and longitudinal-transverse interference response functions have differential sensitivities to physics ingredients such as meson exchange currents.

## The $^{16}$O(e,e'p) Experiment

The initial goal of the experiment is to separate three of the four unpolarized nuclear structure functions: $R_L + (v_{TT}/v_L)R_{TT}, R_T$ and $R_{LT}$ in $^{16}$O at 400±50 MeV/c of internal momenta and a four-momentum transfer of 0.56 (GeV/c)$^2$. The three-momentum transfer is large enough (808 MeV/c) so that significant spatial resolution is obtained while the energy transfer of 312 MeV is still within the regime where proton final state interactions are quite well under control. The structure function separation requires three in-plane measurements. For 3.5% statistics in each of the three cross sections (which allow $R_L + (v_{TT}/v_L)R_{TT}, R_T$ and $R_{LT}$ to be determined to 27%, 15% and 8% respectively once allowance is made for for additional 2% systematic uncertainties) a relatively modest amount of beam time ($\sim$ 800 hrs., see below) will be required. We assume that measurements of the structure functions at lower $|\vec{k}|$ will have been performed at existing laboratories and that they have the required precision. If not, then we would also perform lower $|\vec{k}|$ measurements as part of, or as a prelude to, the experiment proposed here.

Following the successful completion of these first measurements, we would then proceed to a more extreme kinematical situation by increasing the four-momentum transfer to 1.48 (GeV/c)$^2$. This results in greatly increased spatial resolution ($|\vec{q}| = 1463$ MeV/c) and much larger outgoing proton energies ($\omega = 812$ MeV) along with a considerably wider range of missing energies to explore. However, the much lower counting rate at backward angles appears to make separation of $R_T$ impractical; at this higher $Q^2$ we will content ourselves with separation of $R_{LT}$ only. On the other hand, the lower $Q^2$ measurement may indicate considerably larger high-momentum components in the p-shell states than predicted by a Woods-Saxon wavefunction. For this reason, and to allow for the possibility of surprisingly large modifications of the relevant electromagnetic current at the higher $Q^2$, we would make a short (200 hour) exploratory measurement at the backward angle at $Q^2 = 1.48$ G2.

The extension to higher momentum transfer allows several additional aspects of the problem to become accessible: Is the $Q^2$ dependence that of the electron-proton cross section? Is the same $Q^2$ dependence obtained for $R_{LT}$ as for the sum of the other three response functions? Is a transition to a relativistic treatment of the FSI required? At fixed $|\vec{k}|$, to what extent are the differences between this and the lower $Q^2$ measurement explicable in terms of $\sigma_{ep}$ and FSI?, that is, to what extent are other, non-quasielastic reaction

processes present? We already have strong evidence from existing (e,e'p) data[11] that other processes do play a significant role, even at the maximum of the quasielastic peak. In figure 5 are shown missing energy spectra from the $^{12}$C(e,e'p) reaction measured at MIT-Bates for $|\vec{q}| = 600$ and 800 MeV/c. Note the population of the missing energy continuum. Although the origin of this strength is presently unknown, calculations of various FSI effects (two-body NN scattering, intranuclear cascades) can account for only a small fraction ($\sim 10\%$) of the continuum yield. Furthermore, the existence of an additional reaction process of *purely transverse character* in the missing energy continuum has recently been observed in a longitudinal/transverse separation of the $^{12}$C(e,e'p) reaction at MIT-Bates.[12] The kinematics of $|\vec{q}| = 400$ MeV/c and $\omega = 120$ MeV correspond to a point nearly at the maximum of the quasielastic peak. The presence of an additional process is clear from the observation that $R_L$ is consistent with zero for $E_m > 45$ MeV while $R_T$ remains non-zero out to the highest measured missing energies. It is important to realize that final state interactions of the knocked-out proton are unable to produce anywhere near such a large differential effect between the two response functions. Their difference starts increasing above $E_m = 28$ MeV, the threshold for two-nucleon emission. A recent measurement of $^{12}$C(e,e'p) at NIKHEF[13] confirms the increased transversality and its missing energy dependence. The measurements we propose here on oxygen would make large variations in the various "ingredients" of the problem which, along with separation of some of the structure functions, should provide valuable new insight into the (e,e') reaction mechanism.

The kinematics for our measurements are given in tables 1 and 2. In addition to studying the transitions to the $1p_{3/2}$ and $1p_{1/2}$ hole states, we will explore the continuum to 300 MeV as well, since this is where much of the high-momentum strength is expected to lie.[7] "Perpendicular" kinematics were chosen (i.e. $\vec{k}$ nearly perpendicular to $\vec{q}$) so that $R_{LT}$ could be determined by the difference of two cross sections obtained at $\phi_x = 0°$ and $\phi_x = 180°$. A third measurement at a backward electron scattering angle is then required to separate $R_T$. This will only be done for the p-shell states; the estimates indicate that the cross section at backward angles for the continuum is so small that the measurement appears to become impractical for a first experiment. However, we would still like to make a brief exploration of the continuum at the back angle to characterize the magnitude of the cross section and to allow for the possibility of an unexpectedly large yield.

| $\lvert\vec{q}\rvert$ (MeV/c) | $\omega$ (MeV) | $x_B$ | $\lvert\vec{k}\rvert$ (MeV/c) | $\lvert\vec{p}_f\rvert$ (MeV/c) | $T_p$ (MeV) | $\theta_{pq}$ (deg.) |
|---|---|---|---|---|---|---|
| 808 | 312 | 0.948 | 500 | 794 | 291 | 36.4 |
| 1463 | 812 | 0.972 | 500 | 1452 | 791 | 19.7 |

**Table 1.** *Kinematic quantities for $^{16}O(e,e'p)$ measurements at low and high $Q^2$. The Bjorken scaling variable $x_B = q_\mu^2/2M_p\omega$ and $\theta_{pq}$ is the angle between $\vec{q}$ and the detected proton.*

Several factors govern the choice of kinematics. The uncertainties in extracting the longi-

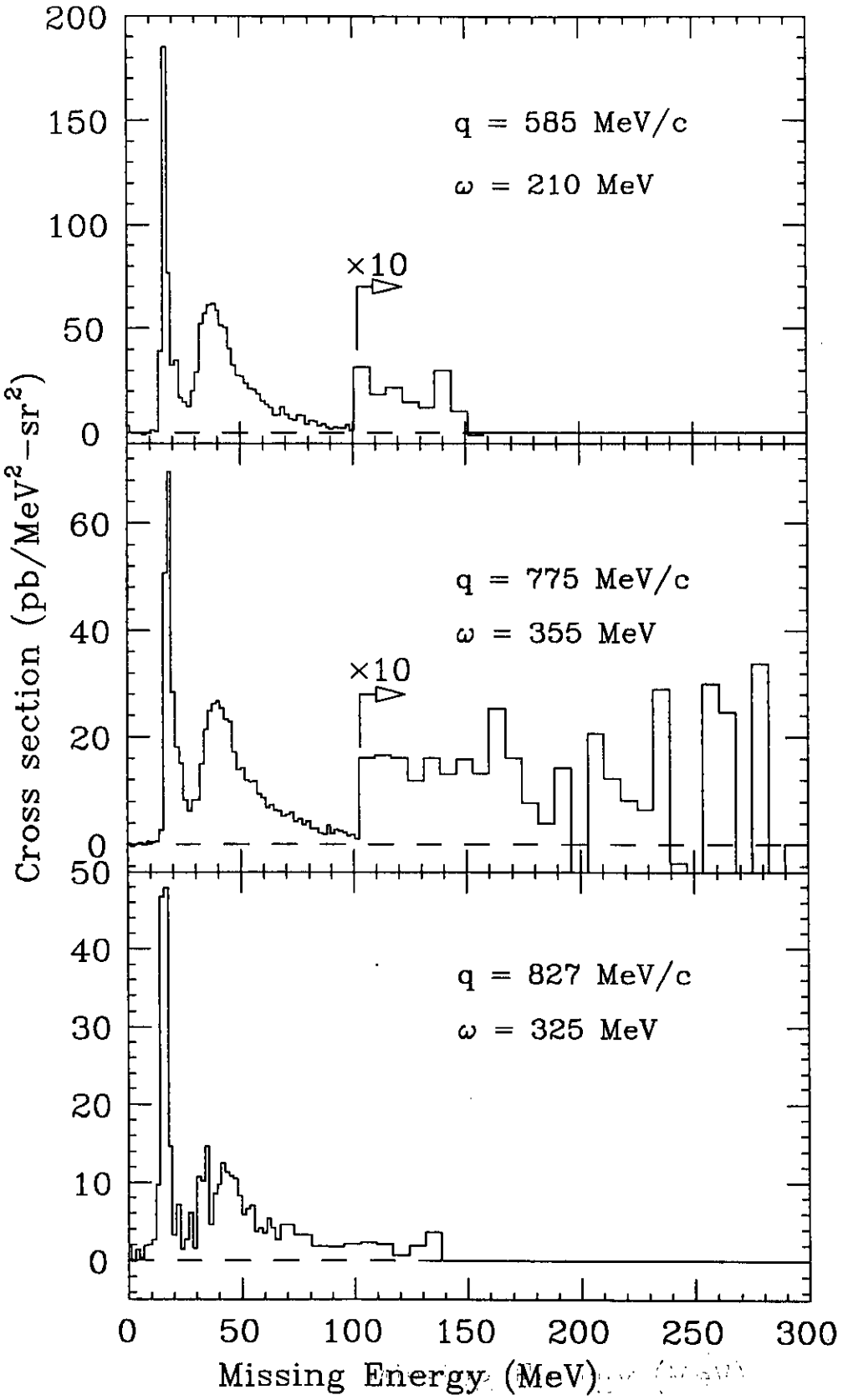


**Figure 5.** *Missing energy spectra from $^{12}C(e,e'p)$ measured at MIT-Bates.*

| Kin. | $E_0$ (GeV) | $E_f$ (GeV) | $\theta_e$ (deg.) | $\theta_q$ (deg.) | $\theta_p$ (deg.) | $\phi_x$ (deg.) |
|---|---|---|---|---|---|---|
| $Q^2 = 0.56$ (GeV/c)$^2$ | | | | | | |
| 1 | 3.45 | 3.14 | 13.0 | 61.0 | 24.6 | 0.0 |
| 2 | 3.45 | 3.14 | 13.0 | 61.0 | 97.3 | 180.0 |
| 3 | 0.71 | 0.40 | 88.6 | 29.7 | 66.1 | 180.0 |
| $Q^2 = 1.48$ (GeV/c)$^2$ | | | | | | |
| 1 | 4.00 | 3.19 | 19.62 | 47.0 | 27.3 | 0.0 |
| 2 | 4.00 | 3.19 | 19.62 | 47.0 | 66.7 | 180.0 |
| 3* | 1.212 | 0.40 | 121.9 | 13.4 | 33.2 | 180.0 |

**Table 2.** *Kinematics for determination of $R_T, R_L + R_{TT}$ and $R_{LT}$ in $^{16}O(e,e'p)$ for $|\vec{k}|$=400 MeV/c in "perpendicular" kinematics at the lower $Q^2$. At the higher $Q^2$, only $R_{LT}$ will be separated unless the exploratory investigation at kinematics 3* indicates the practicality of a more extensive measurement. Each of the kinematics achieves the conditions given in Table 1.*

tudinal and transverse response functions are reduced by choosing a large lever arm (i.e. a large difference in electron scattering angles). A forward electron angle requires high incident energy to achieve the desired momentum transfer. Maximum beam energies of 3.4 and 4.0 GeV were chosen so that one could go as forward as possible (at a given $|\vec{q}|$) with the electron spectrometer. Small electron scattering angles facilitate the L/T separation as mentioned above and increase count rates since the Mott cross section is very forward peaked. This is especially important since much of the phase space sampled at the forward angles will have to be restricted by kinematic cuts so that the structure functions are averaged over the same range as in the backward electron angle measurement. For example, 10% momentum acceptance in the electron spectrometer, $\omega = 312 \pm 155$ MeV at the forward angle and only 312±20 MeV at the backward one. It is crucial that the three quantities $\vec{q}$, $\omega$ and $\vec{P}_r(= -\vec{k})$ be sampled in as nearly identically as possible in each of the cross section measurements from which response functions are to be extracted.

The experiment will employ the two Hall A High Resolution Spectrometers in their "standard" configuration, i.e. 8 msr solid angles and 10% momentum acceptances. The proposed focal plane instrumentation package[14] meets all the resolution and particle ID requirments of this experiment.

The (e,e'p) cross section varies rapidly with some of the experimental quantities (especially $\theta_e$ at forward angles) so uncertainties in these quantities must be kept acceptably small. In table 3 the derivatives $\sigma^{-1}(\partial\sigma/\partial x_i)$ are listed where $x_i = \{E_b, \theta_b, \phi_b, E_e, \theta_e, \phi_e, \theta_p, \phi_p\}$

and the subscripts 'b', 'e' and 'p' refer to the beam, scattered electron and detected proton respectively. The IA cross section with Woods-Saxon $1p_{1/2}$ and $1p_{3/2}$ wavefunctions was employed in the computer code SIGEEP [15] to compute $\sigma$(e,e'p)for the two kinematics at $Q^2 = 1.48$ (GeV/c)$^2$. Note that the cross section can change by several tens of percent over one degree in some cases. It is assumed that all energies/momenta can be determined to $1\times10^{-4}$ and that the beam positioning and definition of the spectrometer central angles are accurate to 0.1 mrad. Simply positioning a spectrometer with this accuracy is necessary but not sufficient, one must also know how the spectrometer maps the solid angle onto its focal plane with similar accuracy. Furthermore, it is the *absolute* as well as the relative energies which must be well-known to avoid unacceptable errors in an L/T separation. The high quality of the Hall A spectrometers should produce uncertainties in $\sigma_1 and \sigma_2$ of 0.5% and 1.0% from systematic effects. These lead to uncertainties in the separated structure function $R_{LT}$ of 2.5% at this $Q^2$. Note that the structure function exhibits fairly strong 'error amplification', for this reason statistical uncertainties also need to be kept small if meaningful determination of the structure functions is to be achieved.

| Variable | Kin. I | Kin. II |
|---|---|---|
| $E_0$ | 0.5/MeV | 1.4/MeV |
| $\phi_b$ | 0.05/deg. | 0.05/deg. |
| $\theta_b$ | 40.3/deg. | 90.2/deg. |
| $E_f$ | 0.6/MeV | 1.7/MeV |
| $\phi_e$ | 0.02/deg. | 0.04/deg. |
| $\theta_e$ | 37.3/deg. | 55.0/deg. |
| $\phi_p$ | < 0.01/deg. | <0.01/deg. |
| $\theta_p$ | 25.5/deg. | 36.1/deg. |

**Table 3.** *Absolute values (in %) of fractional derivatives $\sigma^{-1}$ $(\partial\sigma/\partial x_i)$ of the coincidence cross section with respect to energies and angles for the $Q^2 = 1.48$ $(GeV/c)^2$ part of the $^{16}O(e,e'p)$ experiment. Here, the $\theta_i$ $(\phi_i)$ represent horizontal (vertical) angles.*

Our target requirements can be met with a vertically oriented cylindrical flowing water target. In order to achieve our maximum luminosity of 50 $\mu$A-g/cm$^2$, we need a 500 mg/cm$^2$ target with 100 $\mu$A beam intensity. Therefore, the cylinder will be of 0.5 cm diameter and have 2 micron (1.6 mg/cm$^2$) thick Havar walls. The total wall thickness will be less than 1% of the target thickness. The tensile stress on the walls will be 15,000 psi; Havar has a yield strength of 300,000 psi. This cylinder should be stiff enough to eliminate target thickness fluctuations. The thickness of a cylinder is position dependent. Therefore, in order to reduce effective target thickness fluctuation due to beam wandering to less than $10^{-3}$, we must control the beam position to 100 microns.

For a given pair of scattering angles, the total energy loss for all three particles (initial and final electrons and the proton) will be a function of the interaction vertex. For

the worst case when both spectrometers are at forward angles ($\theta_e = 13°, \theta_p = 26.4°$), the mean of the total energy loss will vary between 1 and 2 MeV. We will use the $y_{tgt}$ resolution of the spectrometers to reduce this energy loss uncertainty to 700 keV (including straggling). When both spectrometers are at large angles, we will also be able to use the HRS[2] $y_{tgt}$ resolution to improve the signal-to-noise by eliminating events coming from different interaction vertices.

A 100 $\mu$A beam will deposit 100 Watts in a 500 mg/cm$^2$ target. If the beam spot is $0.1 \times 0.1$ cm$^2$, then the beam heating will be $2 \times 10^4$ W/gm. If the target does not circulate, then this will cause a temperature rise of $5 \times 10^3$ degrees/sec. To reduce this temperature rise to 5 degrees/sec, the flow rate must be $10^3 \times 0.1$ cm/sec or 1 meter per second. This flow rate should be readily achievable.

Since a water target contains hydrogen, we are able to acquire a prescaled fraction of the $^1$H(e,p) and $^1$H(e,e$'$) events continuously during the experiment to provide absolute calibrations of the target and the individual spectrometers. We will measure the $^1$H(e,e$'$p) reaction before and after the data taking to absolutely calibrate the coincidence setup.

## Count Rate Estimates

The experiment has been simulated using the computer code MCEEP developed at CEBAF by P. Ulmer. Realistic counting rates are obtained since the Monte-Carlo includes all effects of averaging over finite acceptances, non-uniform weighting because of variations in cross section etc. Furthermore, the code allowed kinematic cuts to be placed on the Monte-Carlo data so that we can obtain the best possible matching between the various measurements from which response functions are extracted. It is possible to obtain rather good matching as the histograms of recoil momenta in figures 6 and 7 indicate. Similar quality is obtained for $|\vec{q}|$ and $\omega$. Of course, the sampling at each kinematics can never be made truly identical so that a detailed comparison with theory can only be made after the theoretical calculation has been averaged over the finite acceptances of the instruments.

The counting rates for the experiment were calculated assuming that each spectrometer has 10% momentum acceptance, an 8 msr. solid angle and that the accelerator can provide up to a 200 $\mu$A beam. Singles rates of electrons and protons were derived from the (e,e$'$) and (e,p) cross sections given by the computer codes QFS and EPC.[16] These results are shown in figures 8–10. The EPC code was also used to calculate the $\pi^-$ yield in the electron arm and the $\pi^+$ yield in the proton arm. The only significant yield of pions is in the electron spectrometer at the backward angle. Here, the $\pi^-/e^-$ ratio is about 6:1, a situation easily handled by the Cherenkov and shower counters in the detector package.

The impulse approximation form of the (e,e$'$p) cross section employing Woods-Saxon $1p_{3/2}$ and $1p_{1/2}$ wavefunctions was used for the coincidence rate from these discrete states. The Van Orden calculation of $n(k)$ using the Sprung potential represents a resonable average of the various calculations available and it, along with the assumption that the continuum strength is uniformly distributed over 300 MeV of excitation energy, was used to estimate the count rates in the continuum. The off-shell electron-proton cross section "CC1" of deForest[17] was employed in all the estimates. A 50% attenuation of the protons via FSI was allowed for.

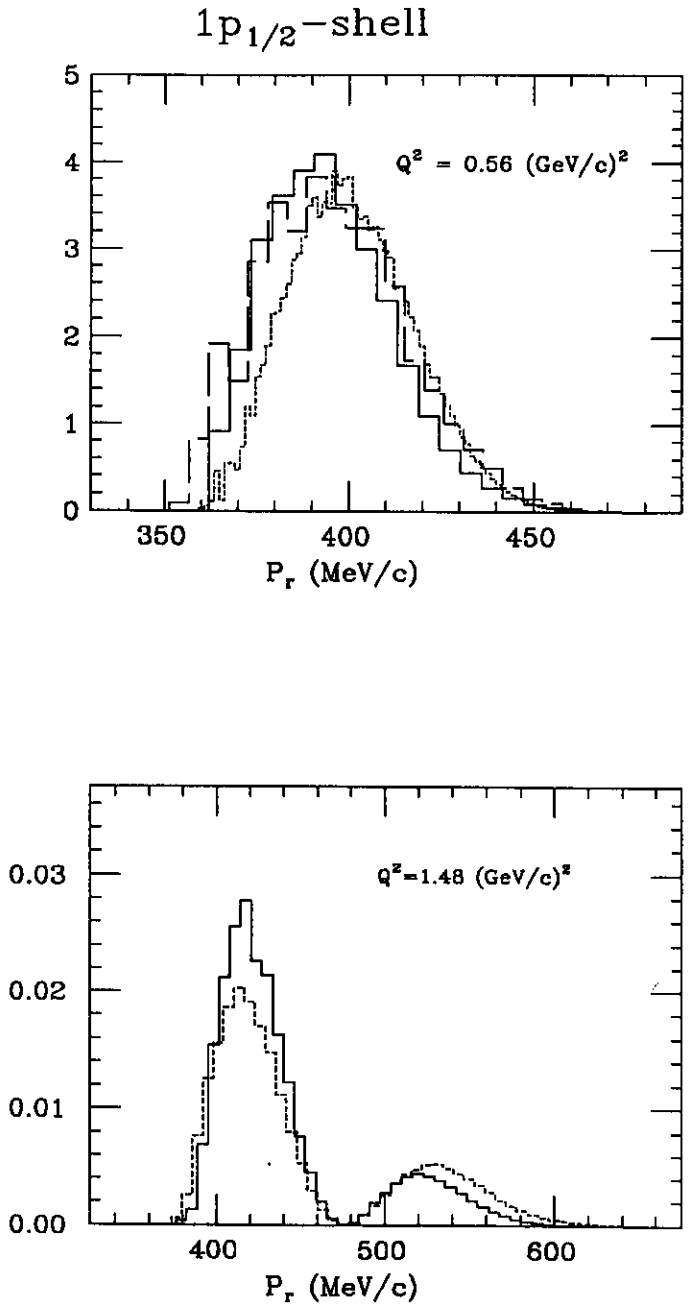


**Figure 6.** *Monte-Carlo result for the sampling of recoil momenta for the* $1p_{1/2}$ *state. The upper plot shows the three kinematics at* $Q^2 = 0.56$ *(GeV/c)*$^2$ *while the lower one displays the result for the two kinematics at 1.48 (GeV/c)*$^2$.

The total time required for the $1p_{1/2}$ state at the $Q^2 = 0.56$ (GeV/c)$^2$ point is based on measuring each of the three cross sections to 3.5% statistical uncertainty. Earlier studies[18] have shown that we can expect an additional 1.5–2% systematic uncertainty from imprecise knowledge of scattering angles, momenta etc (these results were also summarized above). If each of the three cross sections has a total uncertainty of 5%, the structure functions $R_L + (v_{TT}/v_L)R_{TT}$, $R_T$ and $R_{LT}$ for the $1p_{1/2}$ state will be known to 27%, 15% and 8% assuming that their relative sizes are properly given by the off-shell e-p cross section of DeForest.[17] Note that the $1p_{3/2}$ state has about twice the cross section

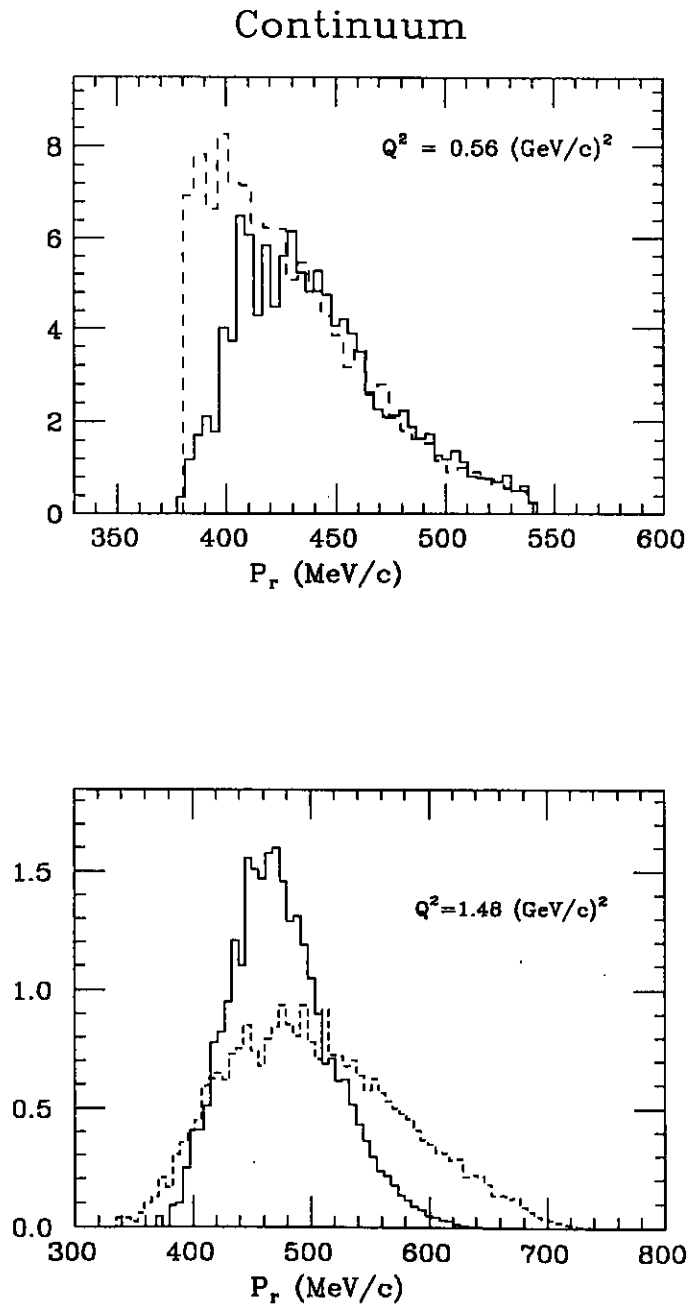


**Figure 7.** *Monte-Carlo result for the sampling of recoil momenta for the first 150 MeV of the missing energy continuum. The upper plot shows the two kinematics at $Q^2 = 0.56$ $(GeV/c)^2$ while the lower one displays the result for the two kinematics at 1.48 $(GeV/c)^2$.*

of the $1p_{1/2}$ state so that the statistical errors for it will be smaller by $\sqrt{2}$.

A 1 MeV excitation energy bin ($\Delta\epsilon_x$) was assumed for the bound states so, considering that all the true coincidences will lie in this bin, the signal-to-noise ratio is greatly increased over the value based on the raw singles rates since the accidental rate for this bin is:

$$R_a = \frac{R_e R_p \Delta t}{df} \frac{\Delta\epsilon_x \Delta E_<}{\Delta E_f \Delta T_p} \quad , \tag{7}$$

where $\Delta E_<$ is the smaller of the electron final energy ($\Delta E_f$) and proton kinetic energy ($\Delta T_p$) acceptances. Note the the $1p_{3/2}$ and $1p_{1/2}$ states are only separated by 6 MeV so

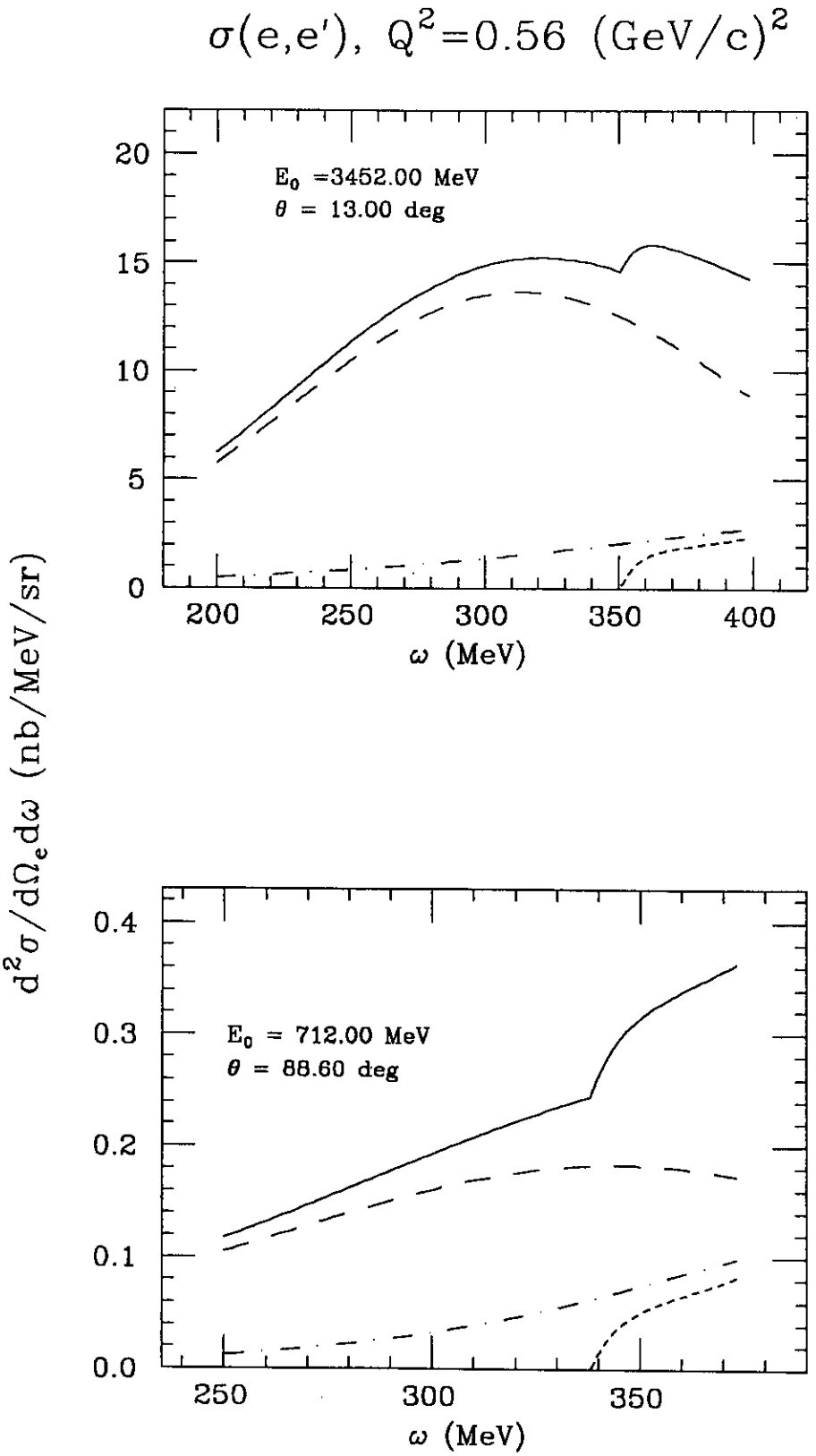


**Figure 8.** *The (e,e′) cross section for the two electron kinematics at $Q^2 = 0.56$ $(GeV/c)^2$. The dashed, dot-dashed and short-dashed curves show the contributions from quasifree knockout, two-nucleon knockout and $\Delta$ excitation respectively.*

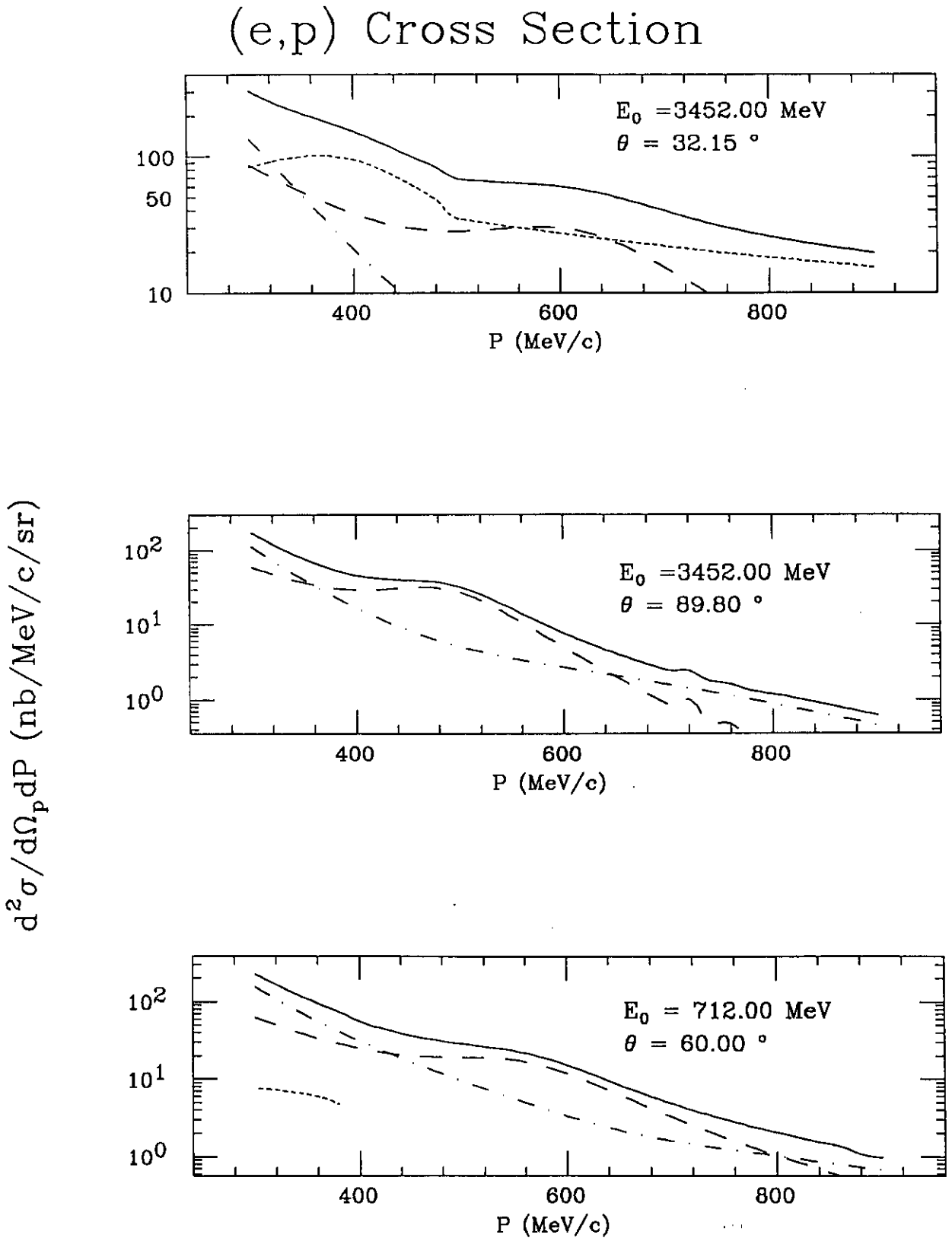


**Figure 9.** The (e,p) cross section for the three proton angles at $Q^2 = 0.56\,(GeV/c)^2$. The dot-dashed, dashed and short-dashed curves show the individual contributions from quasifree knockout, two-nucleon knockout and $\Delta$ excitation respectively.

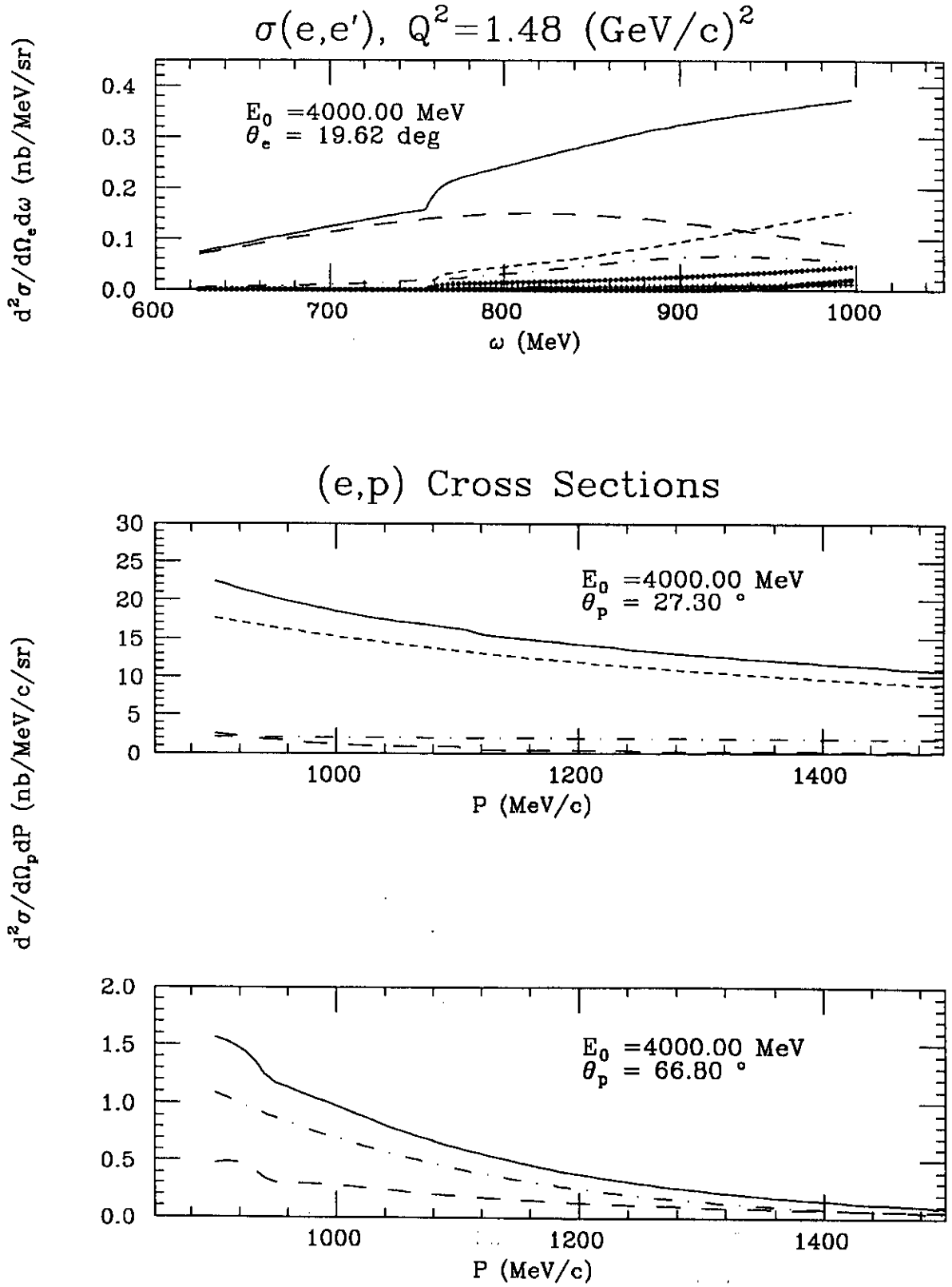


**Figure 10.** *a) The (e,e′) cross section and the (e,p) cross section for the two proton angles at $Q^2 = 0.56$ (GeV/c)$^2$. The curves have the same meaning as in figures 8 and 9.*

data on both will be acquired simultaneously. Therefore, the total time for these two states is that required for the weaker $1p_{1/2}$ state. The cross sections and rates are tabulated in table 4.

## Summary

CEBAF will open up a new window on the high-momentum/short-distance structure of nuclei. The experiment proposed here can accurately probe this new regime of nuclear physics. Counting times seem to be quite manageable. Accuracy and resolution requirements are compatible with the Hall A instrumentation.

Such measurements can provide important tests not only of nuclear structure models but also of models for the underlying nucleon-nucleon interaction giving rise to the short-range correlations. The calculations presently available are based on non-relativistic potential models. Are they appropriate at momentum transfers $> 1$ GeV and distances smaller than the nucleon radius? Are significant contributions present from other, non-quasielastic reaction processes? These are some of the questions we wish to address.

| Kin. | $\sigma$(e,e′) nb/MeV/sr | $\sigma$(e,p) nb/MeV/c/sr | $\sigma$(e,e′p) nb/MeV/sr$^2$ | I·t $\mu$A·g/cm$^2$ | $R_e$ sec$^{-1}$ | $R_p$ sec$^{-1}$ | $R_c$ hr$^{-1}$ | S/N | Time hours |
|---|---|---|---|---|---|---|---|---|---|
| $1p_{1/2}$ knockout at $Q^2 = 0.56$ (GeV/c)$^2$ | | | | | | | | | |
| 1 | 15 | 28 | $7.1\times10^{-4}$ | 5 | 5625 | 21,000 | 7.7 | 0.9 | 222 |
| 2 | 15 | 1.0 | $2.9\times10^{-3}$ | 5 | 5625 | 750 | 31.3 | 106 | 26 |
| 3 | 0.2 | 2.5 | $4.7\times10^{-5}$ | 30 | 495 | 11,250 | 3.1 | 7.8 | 302 |
| TOTAL: 550 | | | | | | | | | |
| continuum to 150 MeV at $Q^2 = 0.56$ (GeV/c)$^2$ | | | | | | | | | |
| 1 | 15 | 114 | $1.9\times10^{-5}$ | 1.5 | 590 | 1280 | 0.90 | 0.45 | 215 |
| 2 | 15 | 40 | $6.4\times10^{-5}$ | 6.3 | 2460 | 1875 | 12.2 | 0.74 | 79 |
| TOTAL: 294 | | | | | | | | | |
| **GRAND TOTAL: 844** | | | | | | | | | |
| $1p_{1/2}$ knockout at $Q^2 = 1.48$ (GeV/c)$^2$ | | | | | | | | | |
| 1 | 0.25 | 12 | $1.0\times10^{-5}$ | 20 | 2640 | 62,250 | 1.3 | 0.7 | 193 |
| 2 | 0.25 | 0.12 | $3.9\times10^{-5}$ | 50 | 6600 | 2040 | 12.6 | 83 | 64 |
| 3* | 0.006 | 0.77 | $1.0\times10^{-7}$ | 50 | 23 | 9020 | 0.01 | 0.9 | 200 |
| TOTAL: 457 | | | | | | | | | |
| continuum to 300 MeV at $Q^2 = 1.48$ (GeV/c)$^2$ | | | | | | | | | |
| 1 | 0.25 | 18 | $6.3\times10^{-7}$ | 0.5 | 75 | 1860 | 1.2 | 0.6 | 921 |
| 2 | 0.25 | 1.2 | $2.5\times10^{-6}$ | 15 | 2250 | 3710 | 72 | 2.4 | 150 |
| TOTAL: 1071 | | | | | | | | | |
| **GRAND TOTAL: 1528** | | | | | | | | | |

**Table 4.** *Count rate estimates for $^{16}O$(e,e′p) $1p_{1/2}$ proton knockout and exploration of the continuum over 150 MeV at $Q^2 = 0.56$ (GeV/c)$^2$ and to 300 MeV at $Q^2 = 1.48$ (GeV/c)$^2$. Note that data on the stronger $1p_{3/2}$ state is acquired simultaneously with the $1p_{1/2}$ state. Kinematics 3* is for an exploratory measuement (see text). The coincidence cross section for the continuum is in units of nb/MeV$^2$/sr$^2$.*

## References


[1] S. Turck-Chieze *et al.*, Phys. Lett. **142B**, 145(1984).

[2] M. Bernheim *et al.*, Nucl. Phys. **A375**, 381 (1982).

[3] UNH-NIKHEF-Mainz collaboration (1988).

[4] J.G. Zabolitzky and W. Ey, Phys. Lett. **76B**, 527 (1978).

[5] A.N. Antonov, V.A. Nikolaev and I.Zh. Petkov, Z. Phys. **A297**, 257 (1980).

[6] a) M. Traini and G. Orlandini, Z. Phys. **A321**, 479 (1985);
b) J.W. Van Orden, W. Truex and M.K. Banerjee, Phys. Rev. **C21**, 2628 (1980).

[7] C. Ciofi degli Atti, E. Pace and G. Salmè, Phys. Lett. **141B**, 14 (1984).

[8] $^3$He: C. Marchand *et al.*, Phys. Rev. Lett. **60**, 1703 (1988);
$^4$He: J.M. Legoff *et al.*, Presented at the $4^{th}$ *Workshop on Perspectives in Nuclear Physics at Intermediate Energies* Trieste, Italy (1989).

[9] O. Benhar, *Research Program at CEBAF II*, (1986).

[10] P.H.M. Keizer *et al.*, Phys. Lett. **197B**, 29 (1987).

[11] L. Weinstein *et al.*, MIT preprint, submitted to Phys. Rev. Lett. (1989).

[12] P.E. Ulmer *et al.*, Phys. Rev. Lett. **59**, 2259 (1987);

[13] G. van der Steenhoven *et al.*, Nucl. Phys. **A484**, 445 (1988).

[14] J.M. Finn *et al.*, CEBAF Internal Report (1989).

[15] P.E. Ulmer, Computer code SIGEEP (1988).

[16] J.W. Lightbody Jr. and J.S. O'Connell, *Computers in Physics* (1988).

[17] T. DeForest Jr., Nucl. Phys. **A392**, 232 (1983).

[18] R.W. Lourie, *Research Program at CEBAF (III)*, pg. 326 (1988).

Continuous Electron Beam Accelerator Facility

12000 Jefferson Avenue
Newport News, Virginia 23606
(804) 249-7100

**Proposal Number:** PR-89-003

**Proposal Title:** Study of the Quasielastic (e,e´p) Reaction in $^{16}O$ at High Recoil Momenta

**Spokespersons/Contact Persons:** W. Bertozzi, R. Lourie, A. Saha, L. Weinstein

**Proposal Status at CEBAF:**

Approval for 20 days of running.

John Dirk Walecka
Scientific Director